

Chapter 7

HESPERIA Forecasting Tools: Real-Time and Post-Event

Marlon Núñez, Karl-Ludwig Klein, Bernd Heber, Olga E. Malandraki, Pietro Zucca, Johannes Labrens, Pedro Reyes-Santiago, Patrick Kuehl, and Evgenios Pavlos

Abstract Within the HESPERIA Horizon 2020 project, two novel real-time tools to predict Solar Energetic Particle (SEP) events were developed. The HESPERIA UMASEP-500 tool makes real-time predictions using a lag-correlation between the soft X-ray (SXR) flux and high-energy differential proton fluxes of the GOES satellite network. We found that the use of proton data alone allowed this tool to make predictions before any Neutron Monitor (NM) station's alert. The performance of this tool for predicting Ground Level Enhancement (GLE) events for the period 2000–2016 may be summarized as follows: the probability of detection (POD) was 53.8%, the false alarm ratio (FAR) was 30%, and the average warning time (AWT) to the first NM station's alert was 8 min. The developed HESPERIA REleASE tool makes real-time predictions of the proton flux-time profiles of 30–50 MeV protons at L1 and is based on electron intensity measurements of energies from 0.25 to 1 MeV and their intensity changes. The performance was tested by using all historic ACE/EPAM and SOHO/EPHIN data from 2009 until 2016 and has shown that the forecast tools have a low FAR (~30%) and a high POD (63%). Furthermore, two methods using historical data were explored for predicting SEP events and

M. Núñez (✉) • P. Reyes-Santiago
Universidad de Málaga, Málaga, Spain
e-mail: mnunez@uma.es

K.-L. Klein • P. Zucca
Observatoire de Paris, Meudon, France
e-mail: ludwig.klein@obspm.fr

B. Heber • J. Labrens • P. Kuehl
Christian-Albrechts – University of Kiel, Kiel, Germany
e-mail: heber@physik.uni-kiel.de

O.E. Malandraki • E. Pavlos
National Observatory of Athens, IAASARS, Athens, Greece
e-mail: omaland@astro.noa.gr

compared. The UMASEP-10mw tool was developed for predicting >10 MeV SEP events using microwave data. The time derivative of the soft X-rays (SXR) was replaced by the microwave flux density. It was found that the use of SXRs and microwave data produced the same POD ($\sim 78\%$) with the most notable difference being that the use of microwave data does not yield any false alarm. Furthermore, a study was carried out on the possibility for the microwave emissions to be used to predict the spectral hardness of the SEP event and important results were deduced.

7.1 Introduction

Forecasting solar energetic particle (SEP) events is of potential interest for spacecraft and launching operations, and for the assessment of radio wave propagation conditions in the polar ionosphere of the Earth. It will be mandatory for human spaceflight beyond low-Earth orbit, especially outside the Earth's magnetosphere. Besides predicting SEP events in general, the prediction of particularly energetic SEPs is a second aim of forecasting, because they penetrate deeper into the terrestrial atmosphere and contribute to the radiation dose aboard aircraft.

Operational real-time SEP forecasts are currently supported by empirical models which rely on observations of associated solar phenomena, including electromagnetic signatures of SEP acceleration/escape near the Sun and observations at the near-Earth environment (L1 or 1 AU) of energetic particles. In this chapter the two novel real-time SEP forecasting tools developed and operating within the HESPERIA project are presented, based on the University of MALaga Solar particle Event Predictor (UMASEP) (Núñez 2011, 2015) and Relativistic Electron Alert System for Exploration (REleASE) schemes (Posner 2007).

The developed and operational HESPERIA UMASEP-500 tool makes real-time predictions of the occurrence of Ground Level Enhancement (GLE) events, from the analysis of soft X-ray (SXR) and differential proton flux measured by the Geostationary Operational Environmental Satellites (GOES) satellite network. Using near-relativistic as well as relativistic electrons as precursors for the arrival of energetic protons, the developed HESPERIA REleASE tools make real-time predictions of the proton flux-time profiles of 30–50 MeV protons at L1. Furthermore, two methods using historical data explored under the HESPERIA project for predicting SEP events are presented and compared. We have tested if the UMASEP scheme can be improved using microwave observations and also studied if the microwave emissions can be used to predict the spectral hardness of the SEP event and important results are deduced.

The first two sections of the chapter are dedicated to the investigations of whether historical microwave emissions can be used in the forecasting of SEP events (Sect. 7.2 and 7.3), whereas the two following sections describe the real-time HESPERIA SEP forecasting tools, using the REleASE and UMASEP proven concepts (Sect. 7.4 and 7.5). Concluding remarks as well as future possibilities are given in Sect. 7.6.

7.2 Predicting SEP Event Onsets from Historical Microwave Data by Using the UMASEP Scheme

Within the HESPERIA project we tested whether microwave emission could be used in the forecasting of SEP events. This is not possible in real time, because no real-time microwave data are presently provided. However, we attempted a proof-of-concept by using historical SEP events.

The UMASEP forecasting scheme (Núñez 2011, 2015) uses the positive time derivative of the observed SXR flux as an indicator of energy release at the Sun. The SXR burst shows the heating of the corona during a flare. The UMASEP scheme considers that a common positive derivative with the particle flux near Earth, with a suitable time delay, indicates a magnetic connection between the Earth and a site of particle acceleration near the Sun. It is well known (Neupert 1968; Dennis and Zarro 1993; Holman et al. 2011) that hard X-ray (HXR) or microwave bursts, produced by non-thermal electrons in the solar atmosphere through bremsstrahlung and gyrosynchrotron emission (see Chap. 2), have time profiles that mimic the time derivative of the SXR. The reason is a common time evolution of the energy release that goes to the electron acceleration on the one hand and to the heating of the plasma during the related flare on the other. While non-thermal electrons lose their energy rapidly through interactions with the solar atmosphere, the heated coronal plasma cools on much slower time scales, and its time evolution is therefore the integral over the distinct episodes of energy release traced by the non-thermal signatures. So as long as the microwave emission is due to gyrosynchrotron radiation of non-thermal electrons, its time profile can be considered as being close to the time derivative of the SXR profile in the impulsive flare phase.

Ground observations of the whole Sun at microwaves can be conducted with patrol-based antennas. The US Air Force operates the Radio Solar Telescope Network (RSTN) consisting of four stations around the world. These stations observe independently from each other, but with identical equipment at selected frequencies.

The most interesting frequencies for our purpose are 4.995 (henceforth referred to as 5 GHz), 8.8 and 15.4 GHz. The data are publicly available after about 1 year via the National Geophysical Data Center (NGDC).¹ Data from the Nobeyama Radio Polarimeters² (NoRP), (Torii et al. 1979; Nakajima et al. 1985), operated by the National Astronomical Observatory of Japan, were used for checking purposes and to replace RSTN when necessary.

In order to test to which extent microwave data can support the UMASEP scheme, we constructed a continuous time series of RSTN observations during a 13-month long period from December 2011 to December 2012. The observations

¹<http://www.ngdc.noaa.gov/stp/space-weather/solar-data/solar-features/solar-radio/rstn-1-second/>

²<http://solar.nro.ao.ac.jp/norp/html/event/>

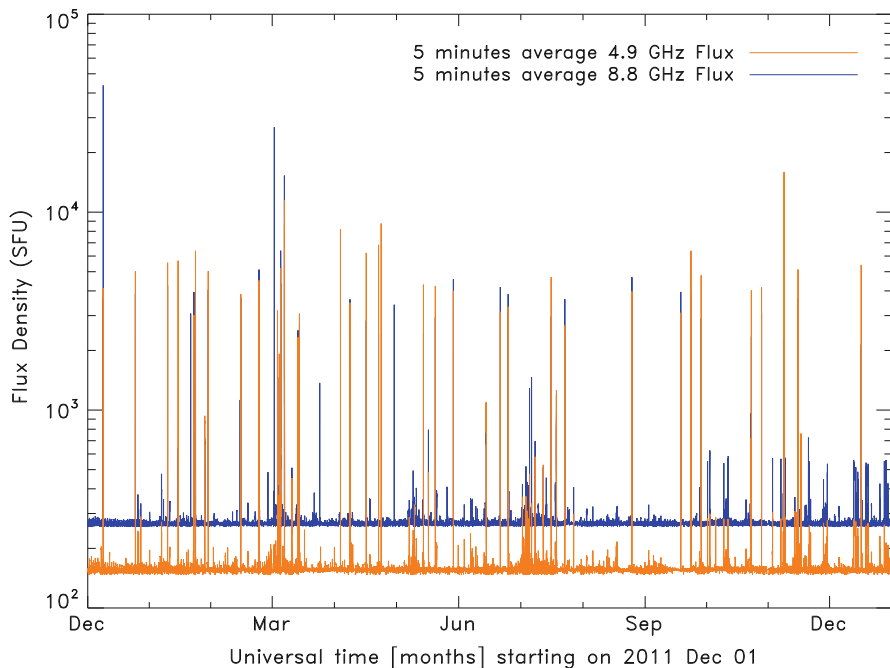


Fig. 7.1 The combined time history of the microwave flux density at two frequencies during the 13 months from 2011 Dec 01 to 2012 Dec 31, constructed from observations of the four RSTN stations

of the individual RSTN stations have a number of problems that needed a careful consideration. We applied a series of standard treatments to remove spikes, data gaps, baseline drifts due to wrong antenna pointing. Then the corrected daily records of the individual stations were combined into the 13-month long time series. A uniform average background was added at each frequency, and smaller flux densities were set to the background value. 5-min integration further smoothes out short-term irregularities that remain after the data cleaning procedure.

Figure 7.1 shows the resulting flux density calculated for the 13 months interval from December 2011 to December 2012. At both frequencies numerous bursts are seen. During this period, nine SEP events were considered as well-connected events and four were considered as poorly connected. An SEP event in the sense used here is an event where the proton intensity at energies above 10 MeV exceeds 10 pfu.

Based on the UMASEP scheme the UMASEP-10mw tool was developed for predicting >10 MeV SEP events using microwave data, the time derivative of the SXR was replaced by the microwave flux density. The UMASEP thresholds were recalibrated. The tool UMASEP-10mw has been developed to be used for calculating the correlation between the solar microwave flux densities at 5 GHz and 8.8 GHz, which are monitored by patrol instruments, and the time derivatives of the near-earth differential proton fluxes measured in different energy channels (i.e. using the GOES satellites).

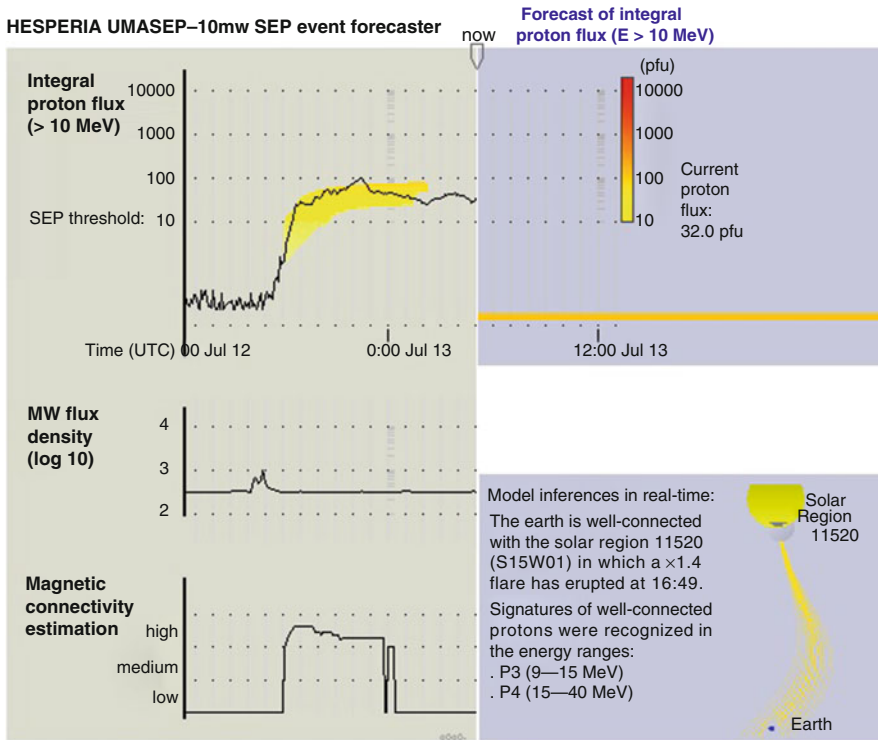


Fig. 7.2 UMASEP-10mw output after processing microwave data at 5 GHz from 2012 July 12 and GOES proton fluxes of >10 MeV energies. The yellow/orange band in the proton intensity plots gives the predicted range, with the colour scale shown by the vertical bar

We illustrate the forecast of the UMASEP-10mw tool using microwave data at 5 GHz for predicting the >10 MeV SEP event.

Figure 7.2 shows the forecast graphical output that an operator would have seen if the UMASEP-10mw tool had processed real-time microwave data on 2012 July 12. The upper time series in both images shows the observed integral proton flux with energies greater than 10 MeV. The current flux is indicated below the label “now” at each image. To the right of this label, the forecast integral proton flux is presented as a yellow/orange-coloured band. The central curve in each panel displays the microwave flux density time profile, and the lower time series shows the magnetic connectivity estimation with the best-connected coronal mass ejection (CME)/flare process zone.

Figure 7.2 also shows the prediction at 18:05 (2012 July 12). This forecast is that an event will start during the following 2 h and reach a peak intensity of 36 pfu 9 (see white section “Automatic forecast”). Below the forecast section, the system also presents the model inference section, which shows that the Earth is well-connected with the solar region 11520. The system also shows that the associated X1.4 flare

took place at S15W01. As time passes, the integral proton flux also rises. At 18:35 UT, the flux exceeds the 10-pfu threshold, which indicates that a proton event is occurring. Note that the well-connected SEP event was successfully forecast 30 min earlier, when the enhancement of the integral proton flux was still weak (1.24 pfu).

To measure the overall performance of this tool, we run the UMASEP forecasting schemes using on the one hand the SXR observations, on the other hand the microwave observations at the two frequencies considered for the aforementioned period. We evaluated two quantities: the probability of detection (POD) is the number of the predicted SEP events divided by that of the SEP events that actually occurred, i.e. nine events in the considered time interval. The false-alarm ratio (FAR) is the number of false predictions over the number of predictions. Seven predictions were triggered when microwaves were used, and eight with SXR. We found that the use of SXR and microwave data produced the same $POD = 77.8\%$ (7/9). The most notable difference is that the use of microwave data does not yield any false alarm. The average warning time (AWT) is slightly higher when microwave observations are used 30.7 min as compared to 26.4 min.

The probabilities of detection used above are adequate to compare the performance of SXR and microwaves within the UMASEP scheme, but overestimate the expected ones: SEP events originating behind the solar limb are undetectable to the UMASEP Well-Connected Prediction model (WCP), because it uses electromagnetic observations from a terrestrial vantage point. This bias affects SXR from GOES and radio observations from ground alike.

A more detailed account of this work is given in Zucca et al. (2017).

7.3 Predicting SEP Energy Spectra from Historical Microwave Data

Depending on their peak intensity and spectral hardness, SEP events constitute different kinds of space weather hazard. Protons and heavy ions at energies between several MeV and several tens of MeV may interact with spacecraft and human beings above low-Earth orbit, and ionize the high polar atmosphere of the Earth. GeV protons create atmospheric cascades down to the Earth and enhanced radiation doses at aircraft altitudes. High intensities in the two energy ranges are not necessarily observed in the same events (Mewaldt et al. 2007). Besides the occurrence, spectral hardness is therefore a space-weather relevant information, and a second goal in SEP forecasting.

It was shown in Grechnev et al. (2015 and references therein) that SEP events above 100 MeV are often accompanied by strong microwave emission well above the average peak frequency of 10 GHz. On the other hand the peak flux density or peak fluence of microwave bursts also show some correlation with the peak intensity of SEPs at tens of MeV (Kahler 1982; Trotter et al. 2015). Chertok et al. (2009) went one step further and suggested that SEP events with hard proton

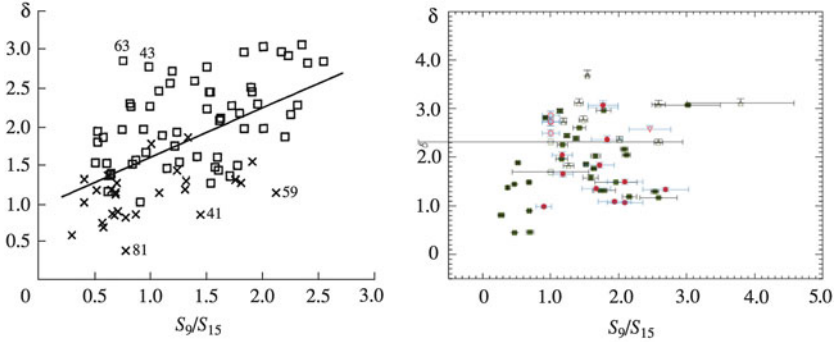


Fig. 7.3 Scatter plots of the spectral hardness of the proton spectrum δ , versus the peak microwave flux density ratio at 8.8 and 15.4 GHz, labelled S_9/S_{15} . (a) Study by Chertok et al. (2009). (b) Present work based on data from GOES integral intensities above 10 MeV and above 100 MeV taken during solar cycles 23 and 24

spectra in space in the 10–100 MeV range tend to be accompanied by microwave bursts where the flux density at the highest frequency continually monitored from ground, which is 15.4 GHz, exceeds the flux density at 9 GHz. The ratio of flux densities at the two frequencies, which is an easily observable parameter, seems to correlate significantly ($r = 0.55$) with the proton spectral hardness during solar cycles 22–23.

We re-examined the relationship during cycles 23 and 24, using the integral proton intensities measured by the GOES. We consider integral intensities above 10 MeV (designated by J_{10} in the following) and 100 MeV (J_{100}) for events associated with activity in the western solar hemisphere, and calculated the ratio

$$\delta = \log_{10} \left(\frac{J_{10}}{J_{100}} \right) \quad (7.1)$$

In Fig. 7.3 the scatter plot between the proton spectral hardness δ and the ratio of peak flux densities at 8.8 and 15.4 GHz derived by Chertok et al. (2009) (a) is compared with our work (b). Both plots suggest a slight trend that SEP events with hard proton spectra are associated with microwave bursts that are stronger at 15.4 than at 8.8 GHz. But the correlation is questionable in cycles 23–24: the linear correlation coefficient of the sample in Fig. 7.3b is 0.26 ± 0.20 in solar cycle 23, and still weaker in solar cycle 24. So we find no convincing correlation that could support a forecasting procedure of spectral hardness of SEPs. We also tested a correlation between spectral hardness and the speed of the associated CME. This was also inconclusive, with a correlation coefficient of 0.15 ± 0.16 in solar cycle 23.

There is a number of reasons why a relationship between the microwave peak frequency and the SEP spectral hardness in the range (10–100) MeV could be masked. One is the likely contribution of different acceleration processes to the SEP

populations (Trottet et al. 2015) and the variation of their contribution with particle energy (Dierckx et al. 2015). If the SEPs above 10 MeV were predominantly accelerated by CME shocks, and those above 100 MeV by flares or similar processes lower in the corona, no direct correlation would be expected. The other reason is that the microwave flux density spectrum depends strongly on the magnetic field strength and orientation in the radio source, which is also not expected to have an effect on the SEPs. Finally there is an interesting hint that radio bursts with relatively high flux density at 15.4 GHz (and flat SEP spectra) were lacking in solar cycle 24. Forecasting schemes can of course use empirical correlations independently of our understanding of the physical relationships. But this does not seem convincing in the present case.

7.4 Predicting 30–50 MeV SEP Events by Using the RELeASE Scheme

The fact that near relativistic electrons (1 MeV electrons have 95% of the speed of light) travel faster than ions (30 MeV protons have 25% of the speed of light) and are always present in SEP events, a forecast of the arrival of protons from SEP events can be based on real-time measurements of near relativistic electrons. The faster electrons arrive 30–90 min before the slower protons at Lagrangian point 1. The Relativistic Electron Alert System for Exploration (RELeASE) forecasting scheme uses this effect to predict the proton flux by utilizing the actual electron flux and the increase of the electron flux in the last 60 min. A detailed description of the RELeASE scheme can be found in (Posner 2007). The original RELeASE code uses real-time electron flux measurements from the Electron Proton Helium Instrument (EPHIN) (Müller-Mellin 1995) on board the Solar and Heliospheric Observatory (SOHO) to forecast the expected proton flux.

RELeASE is based on electron intensity measurements of energies from 0.25 to 1 MeV and their intensity changes. It utilizes an empirical matrix in order to predict the proton intensity 30, 60 or 90 min ahead. Figure 7.4b displays the forecast matrix for one proton channel and the 60-min interval. EPHIN provides realtime data which are used with the RELeASE scheme. One disadvantage of EPHIN data is the limited time coverage in the realtime data of less than 4 h per day. If no realtime data are available as input for the RELeASE scheme, no forecast can be produced. The Electron Proton Alpha Monitor (EPAM) onboard the Advanced Composition Explorer (ACE) was selected to be a good candidate to deliver continuously input for RELeASE because of the nearly full time coverage. EPAM provides realtime electron intensities in a comparable energy range (0.175–0.315 MeV vs. 0.25–1.0 MeV) but in a time resolution of 5 min instead of 1 min.

The forecast depends on the measured electron intensities and their increase. Hence we decided to determine a correlation between the intensities and the increase parameter. Figure 7.4a shows the time profile of EPAM (red) and EPHIN

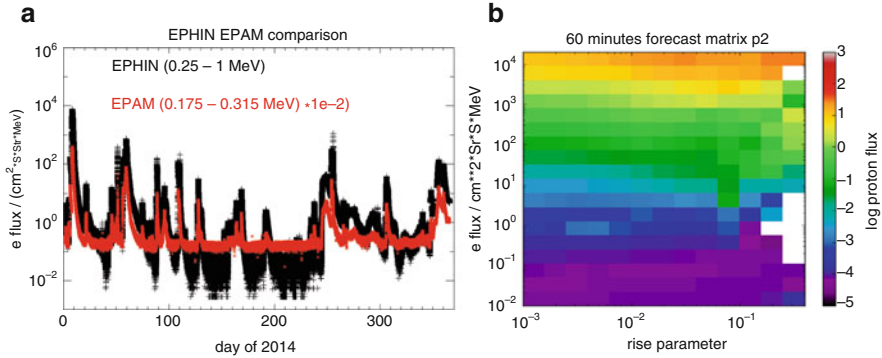


Fig. 7.4 The *left* panel (a) shows the time series of EPHIN (*black*) and EPAM (*red*) electron intensities. The electron intensity measured by EPAM is divided by 10. The *right* panel (b) displays an example of one forecast matrix used within the RELeASE scheme. This Matrix shows the predicted intensity of protons in 1 h as function of the measured absolute electron intensities and the intensity rise parameter

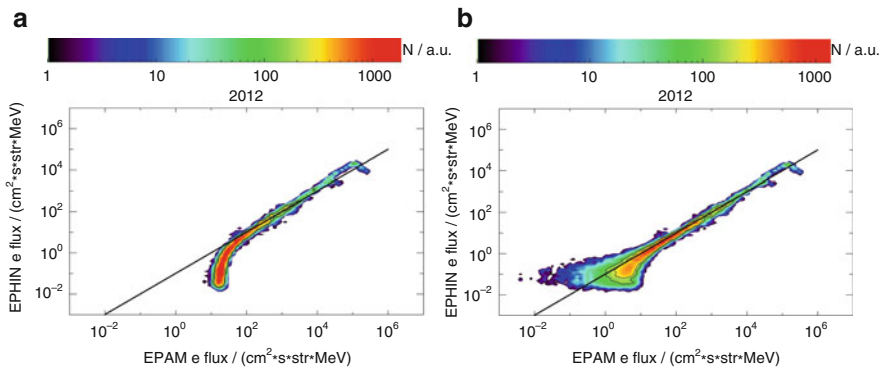


Fig. 7.5 The *left* panel (a) displays 5 min electron intensities of EPAM (*x*-axis) and EPHIN (*y*-axis) plotted against each other. The *right* panel (b) shows the same plot for background subtracted data

(black) electron intensities of 2014. Despite the high background of the EPAM measurements there seems to be a good correlation. If there is an increase in EPHIN electron intensity there is also one in EPAM.

To quantify this correlation Fig. 7.5a shows the EPHIN electron intensity on the *y*-axis plotted against the corresponding EPAM intensities on the *x*-axis. The higher background level of EPAM reflects itself by the nearly vertical line at low EPAM intensities. In order to correct for that we subtracted a background intensity of 18 $(\text{cm}^2 \text{ s sr MeV})^{-1}$ from the EPAM data. The result of this procedure is shown in Fig. 7.5b in the right panel. Despite these differences the EPAM electron intensity is roughly ten times higher as the one determined by EPHIN. This is indicated by the black line showing the function where EPAM intensity is ten times higher than EPHIN intensities.

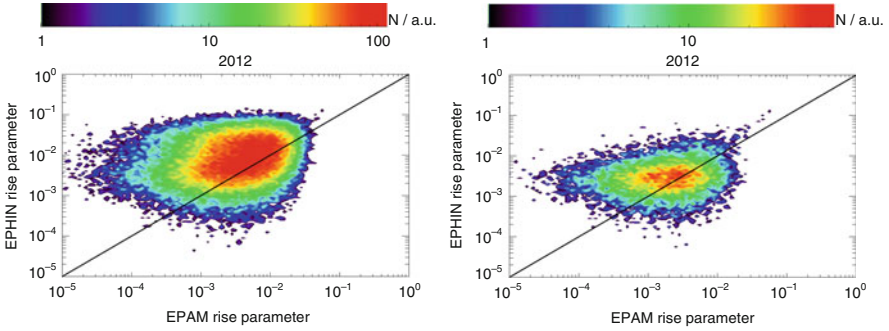


Fig. 7.6 Rise parameter of 5 min electron intensities measured by EPAM (x-axis) and EPHIN (y-axis). The EPAM intensity was background subtracted. The *right* panel displays all data from 2012 while the *left* panel shows only rise-parameters for strong enhanced electron fluxes

From our investigation, we conclude that there is a good correlation for intensities higher than $20 \text{ (cm}^2 \text{ s sr MeV)}^{-1}$. Due to the large background the correlation breaks down for EPAM intensities below $20 \text{ particles (cm}^2 \text{ s sr MeV)}^{-1}$. Since the goal of the REleASE system is to forecast SEP events with high particle fluxes the background uncertainties play a negligible role here. The EPAM intensity in addition was raised to the power of 1.02 to correct for different correlation at very high intensities.

The second parameter used in the REleASE forecast matrices (x-axis) is the intensity rise parameter. This parameter is calculated by linear fits through the logarithmic electron intensities of the last 5–60 min. The maximum of these parameters is transferred to the rise parameter position in the forecast matrices. A comparison of the rise parameters from EPHIN and EPAM is shown in Fig. 7.6. One can see that most of the data points are close to the bisecting line, but do not show a correlation between the rise parameters. If we only take electron fluxes higher than 102 into account, the correlation gets stronger. Due to this and the fact that the forecast matrix in Fig. 7.4 shows a much stronger dependence on the electron intensity we decided to use the uncorrected EPAM rise parameter as input to the REleASE scheme. Figure 7.7 shows an example of an SEP event where the EPHIN based and EPAM based forecasts predicted the real proton flux very accurately.

Since forecasts are made for different time offsets (30, 60, 90 min) and different overlapping energy channels (16–40 and 28–50 MeV), we investigated a suitable forecast condition in combining the different forecasts. We tested different combination of forecasts for different time offsets and found that the following condition delivered the best performance of the forecast systems:

- Alarm: if any forecast $> 10^{-1} \text{ (cm}^2 \text{ s sr MeV)}^{-1}$ and one 30 min forecast $> 10^{-2} \text{ (cm}^2 \text{ s sr MeV)}^{-1}$.
- Event: if real proton flux $> 10^{-1} \text{ (cm}^2 \text{ s sr MeV)}^{-1}$.

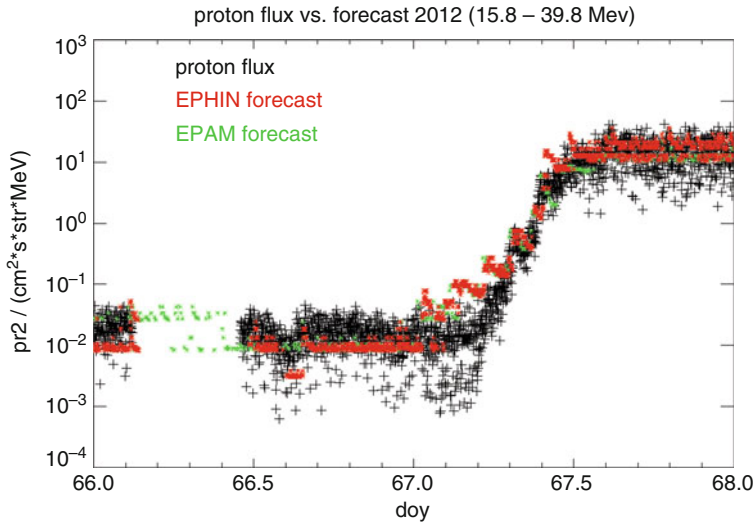


Fig. 7.7 An example of an SEP event where the EPHIN and EPAM based forecasts predicted the real proton flux accurately

Table 7.1 Results of REleASE implementation utilizing either SOHO/EPHIN or ACE/EPAM

	T	M	F	POD (%)	FAR (%)	AWT (min)
EPHIN	24	14	10	63	29	107
EPAM	24	14	13	63	35	123

The performance was tested by using all historic EPAM and EPHIN data from 2009 until 2016. All SEP events of this time period were investigated. The following results for events are possible:

- True forecast (Alarm and Event): T
- Missed event (No/late Alarm and Event): M
- False alarm (Alarm and no Event): F

By using the total number of true forecasts, missed events and false alarms of the analysed time period, it is possible to calculate the Probability of Detection (POD) and False Alarm Ratio (FAR):

- False Alarm Ratio: $FAR = \frac{F}{T+F}$
- Probability Of Detection: $POD = \frac{T}{T+M}$

The results of the described analysis are summarized in Table 7.1.

The described forecast tools have low FARs and sufficient PODs. The tools are publicly available via the HESPERIA project web site. On this web site we provide an e-mail alert system. Interested users are welcome to sign in for this alert system.

7.5 Predicting >500 MeV SEP Events by Using the UMASEP Scheme

Solar energetic particles (SEPs) are sometimes energetic enough and the flux is high enough to cause air showers in the stratosphere and in the troposphere, which are an important ionization source in the atmosphere. >500 MeV solar protons are so energetic that they usually have effects on the ground, producing what is called a Ground Level Enhancement (GLE). One of the goals of the HESPERIA project was the development of a predictor of >500 SEP events at the near-earth (e.g. at geostationary orbit). The implemented predictor, called HESPERIA UMASEP-500, makes a lag-correlation between the SXR flux and high-energy differential proton fluxes of the GOES satellites. When the correlation estimation surpasses a threshold, and the associated flare is greater than a specific SXR peak flux, a >500 MeV SEP forecast is issued.

The lag-correlation is carried out using the High-Energy UMASEP approach explained in Núñez (2015). In this project, this approach uses 1-min SXR and proton data. Firstly, it generates a bit-based time series from the SXR time-derivatives and three bit-based time series from the time-derivatives of each of the P9–P11 channels of the GOES6–GOES15 satellites. The “1s” in each bit-based time series are set when its positive time derivative surpasses a percentage p of the maximum value of the time derivative in the present sequence of size L (beyond which no influence is assumed in the SEP event to be predicted); otherwise, the flux level is transformed into a “0”. To avoid false alarms due to relatively strong fluctuations during periods of low solar activity, a threshold d is necessary, which is the minimum value to consider it as positive fluctuation (i.e., a “1”). This forecasting approach creates a list of *cause-consequence pairs* as follows: it takes the first “1” of the SXR-based time series, and the first “1” of the proton-based time series, to create a *pair*; it then takes the second pair of “1s” in each time series, and thus successively, until all the “1s” of the SXR-based time series are inspected. After following this procedure, if a “1” does belong to any pair, it is classified as an “odd”. For each pair, the *pair separation* between the SXR-based “1” and the proton-based “1” is calculated.

An ideal magnetic connection is detected when a sequence of SXR-based “1s” in a row is followed by a sequence of proton-based “1s” in a row. In an ideal magnetically connected event, all pairs have the same temporal separation, and no odd “1” has been found; in other words, an ideal magnetic connection is detected when all recently-measured strongest rises in the SXR flux are followed, some minutes later (i.e. the lag), by all recently-measured strongest rises in a proton channel. We say that this ideal magnetic connection would have a *Fluctuation Correlation* of 1. In general, we need a formula, described in Núñez (2015), that calculates the Fluctuation Correlation between the bit-valued SXR-based time series and a proton-based time series. A >500 MeV SEP event is triggered when the lag-correlation is greater than a threshold r , and the SXR intensity of the associated flare is greater than a threshold f .

It is important to mention that a >500 MeV SEP event is detected when the integral proton flux surpasses a certain threshold $p_{fu}500$. To calculate this threshold, firstly we had to use the geometrical factors of P9, P10 and P11 proton channels provided by the National Oceanic and Atmospheric Administration (NOAA). Then, we manually varied this threshold to match each >500 MeV SEP event with each GLE event. The study ended with a threshold of 0.8 pfu, which yielded a one-to-one correspondence in 26 of the events of all 32 GLE events within the analyzed period (1986–2016). In 8 cases, a GLE was observed at Earth; however, the enhancement in >500 MeV integral proton flux did not surpass 0.8 pfu. In only one case (see Event 44.5 in Table 7.2) a >500 MeV SEP event took place, which was not observed at the ground.

The UMASEP-500 model's parameter calibration from historical data was an optimization process whose purpose was to obtain a high POD and Advance Warning Time (AWT), and a low FAR. We found that the same thresholds and parameters found for predicting >500 MeV SEP events were also very appropriate to predict GLE events; for this reason, this section also presents a summary of the GLE forecast results. For more information about the GLE forecast results, please consult Núñez et al. 2017.

The original purpose of the HESPERIA UMASEP-500 tool was to correlate SXR with neutron and proton data. We found that the use of proton data alone allowed this tool to make predictions before any Neutron Monitor (NM) station's alert. This satisfactory result became our operational criterion for classifying a GLE forecast as successful. We found that the correlation of SXR and neutron counter data did not trigger any hit additional to those generated using proton data alone. We also found that the use of neutron data provoked the generation of many false alarms due to some quality data problems (mainly spikes) caused by technical issues, such as problems in the neutron sensor tubes and power supplies, among others (Souvatzoglou et al. 2014). Since the use of neutron data did not increment the POD, but did increment the FAR, we decided not to use neutron data for making predictions.

Figure 7.8 presents the forecast output for the >500 MeV and GLE event on October 28, 2003. The upper time series shows the recent >500 MeV proton flux; the predicted flux is presented with a colored curve. The middle time series shows the recent SXR flux. The plot at the bottom of the forecast output presents the empirically-estimated level of magnetic connectivity. The Automatic Prediction section (on the right) presents in red the prediction of the occurrence of the GLE event. Below, the tool presents the details of the associated flare, and the proton channels for which the SXR correlation was found. The small image at the top-right shows the real evolution of the integral proton flux after this prediction. The 1-min real-time forecast outputs of this tool are shown on the website of the HESPERIA project (i.e. <https://www.hesperia.astro.noa.gr/index.php/results/real-time-prediction-tools/umasep>).

The overall prediction performance of event occurrences for the analyzed period (1986–2016) was calculated in terms of POD, FAR and AWT. Table 7.2 presents the list of GLEs, >500 MeV SEP events, and the HESPERIA UMASEP-500's

Table 7.2 HESPERIA UMASEP-500's forecast results of the GLE and >500 MeV SEP events that took place during the analyzed period (1986–2016)

Solar event Event ID	GLE Onset (UTC)	Time	GLE Forecast Result ^a	GLE Forecast Warning Time (min) ^a	>500 SEP Event Onset Time (UTC)	>500 SEP Forecast Result	>500 SEP Forecast Warning Time (min)
GLE-40	25/07/1989	8:50	Miss		9:13	Miss	
GLE-41	16/08/1989	1:25	Hit	20	1:37	Hit	32
GLE-42	29/09/1989	11:40	Hit	6	11:51	Hit	17
GLE-43	19/10/1989	13:00	Hit	8	13:03	Hit	11
GLE-44	22/10/1989	17:55	Miss		17:57	Miss	
Ev-44.5	23/10/1989				12:42	Miss	
GLE-45	24/10/1989	18:18	Miss		18:24	Miss	
GLE-46	15/11/1989	7:00	Miss				
GLE-47	21/05/1990	22:29	Miss		23:02	Miss	
GLE-48	24/05/1990	20:49	Miss		21:06	Miss	
GLE-49	26/05/1990	20:55	Miss		21:10	Miss	
GLE-50	28/05/1990	5:34	Miss				
GLE-51	11/06/1991	2:30	Hit	24	3:18	Hit	72
GLE-52	15/06/1991	8:35	Hit	2	8:40	Hit	7
GLE-53	25/06/1992	20:15	Miss		20:18	Miss	
GLE-54	02/11/1992	3:50	Hit	20	3:24	Hit	28
GLE-55	06/11/1997	12:10	Miss		12:27	Miss	
GLE-56	02/05/1998	13:55	Miss				
GLE-57	06/05/1998	8:25	Miss				
GLE-58	24/08/1998	22:50	Miss				
GLE-59	14/07/2000	10:34	Hit	12	10:36	Hit	14
GLE-60	15/04/2001	13:57	Hit	1	13:57	Hit	1

GLE-61	18/04/2001	2:33	Miss					
GLE-62	04/11/2001	16:55	Miss		16:44		Miss	
GLE-63	26/12/2001	5:39	Miss		6:08		Miss	
GLE-64	24/08/2002	1:23	Hit	13	1:30		Hit	20
GLE-65	28/10/2003	11:17	Hit	9	11:31		Hit	23
GLE-66	29/10/2003	21:02	Hit	3	21:19		Hit	20
GLE-67	02/11/2003	17:27	Hit	3	17:35		Hit	11
GLE-68	17/01/2005	9:52	Miss					
GLE-69	20/01/2005	6:47	Miss		6:46		Miss	
GLE-70	13/12/2006	2:50	Hit	15	2:59		Hit	24
GLE-71	17/05/2012	1:55	Miss		2:07		Miss	

^aHits are predictions that are triggered before the first NM station's GLE alert

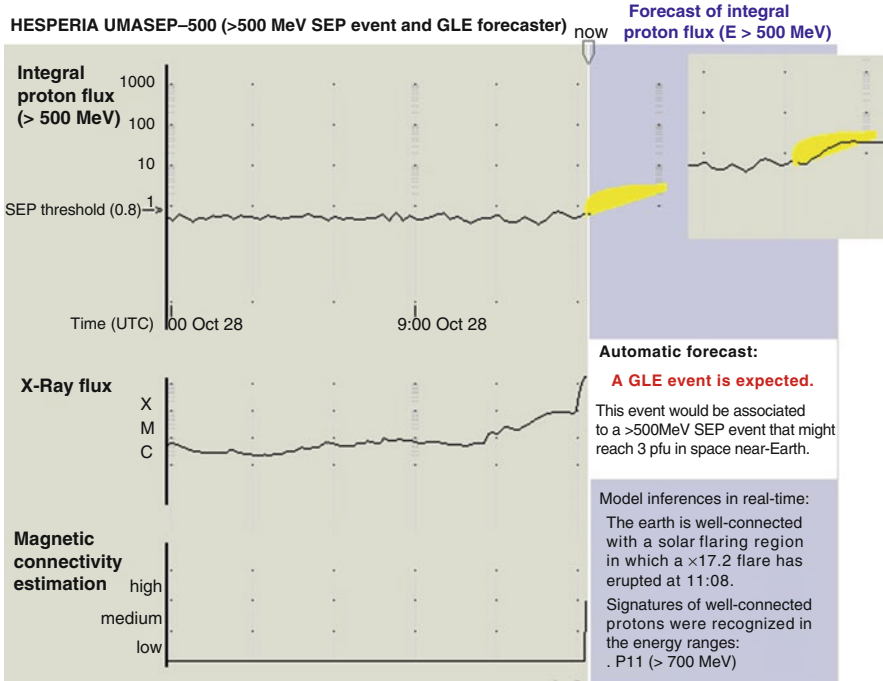


Fig. 7.8 This figure shows the forecast output of HESPERIA UMASEP-500 for the event occurred on October 28, 2003. This prediction, issued at 11:08, was successful because it was issued before the >500 MeV integral proton flux surpassed 0.8 pfu (at 11:31), and before the first NM station's alert, issued at 11:17

prediction results for the events of the analyzed period. Column 1 presents the GLE event ID; column 2 lists the time of the first detection of the event of an NM station; column 3 presents the HESPERIA UMASEP-500 GLE prediction results (hits are those events successfully predicted, and misses are those not-successfully predicted); column 4 lists the warning times (i.e. the temporal difference between the time at which the forecast was triggered by this tool and the time of the first NM station's alert); column 5 lists the time the occurrence of the SEP event (i.e. the time when the >500 MeV proton flux surpassed 0.8 pfu); column 6 presents the SEP prediction results; and, column 7 lists the warning times.

Regarding the prediction of >500 MeV SEP event, the forecast performance results of this tool for the period 1986–2016 may be summarized as follows: the POD was 50% (13/26), the FAR was 31.6% (6/19), and the average warning time to the first NM's alert was 13 min.

Regarding the prediction of GLE events, the forecasting results for the most recent half of the evaluation period (i.e. 2000–2016) may be used to compare UMASEP-500 with those of the GLE Alert Plus. These results may be summarized as follows: the POD was 53.8% (7 of 13 GLE events); the FAR was 30.0% (3/10);

the AWT to the first NM's alert was 8 min; and, the AWT to the GLE Alert Plus's warning was 15 min. The GLE forecasting results for the first half of the evaluation period (i.e. 1986–1999) are summarized as follows: the POD was 31.6% (6 of 19 GLE events); the FAR was 33.3% (3/9); and, the AWT to the first NM's alert was 13.3 min. There are no forecasting results of the GLE Alert Plus for this period.

For the whole evaluation period, the GLE forecasting performance may be summarized as follows: the POD was 40.6% (13 of 32); the FAR was 31.6% (6 of 19); and, the AWT to the first NM's alert was 10.5 min. Note that the FAR of the most recent period is similar to that of the oldest period (30.0% vs. 33.3%); however, the POD of the most recent period (i.e. 53.8%) is better than the POD of the oldest period (i.e. 31.6%). We do not know the reason for the better POD performance in the most recent period; nevertheless, we think that the use of a more recent and refined instrument technology and/or more experienced calibration procedures yields better forecasting performance.

7.6 Concluding Remarks

We experimented the use of microwave time histories in the UMASEP prediction scheme of the occurrence of SEP events. The test run over 13 months shows that microwaves provide a comparable probability of detection, but a reduced false-alarm ratio as compared to the time derivative of the SXR flux, which is used in the traditional UMASEP scheme.

The reduction of false alarms is due to the fact that microwave bursts are signature of non-thermal particle acceleration and are less frequent than the ubiquitous thermal soft X-ray brightenings. This reduces the probability to interpret the chance coincidence between a rise of the radiative signature and the rise of the particle intensity at the spacecraft as an indication of a magnetic connection. The forecasting scheme using microwaves fails when the microwave emission is thermal and slowly rising. This is especially the case when SEP events are related to the eruption of quiescent filaments.

A second test of microwave patrol observations in SEP forecasting was conducted with the aim to predict the hardness of proton spectra using the ratio of peak flux densities at 15.4 and 8.8 GHz: the expectation was to find a preferential association of hard proton spectra with microwave bursts that are particularly strong at 15.4 GHz, as had been shown in previous activity cycles (Chertok et al. 2009). We were unable to confirm this expectation: we found no significant correlation between the proton spectral hardness and the microwave flux density ratio. The intrinsic variations from event to event are much stronger than any underlying trend that might exist.

The radio patrol observations used by our study are carried out with rather simple patrol instruments, which monitor the whole Sun flux density using parabolic antennas with a typical size of ~ 1 m. Such data are presently not provided in real time, but there is no technical obstacle to do so. But the results of our test run for the

prediction of well-connected SEP events show that microwave observations have the potential to improve SEP forecasting. An interesting perspective could be the combination of the REleASE and UMASEP forecasting schemes, because, on one hand they could correlate rises between microwaves at the Sun and electrons, and on the other hand, forecasts may be provided for those SEPs whose parent solar event is behind the limb. This combination of schemes could bring a major gain in advance warning time.

The HESPERIA REleASE tools make real-time predictions of the proton flux (30–50 MeV) at Lagrangian point 1 and are available via the HESPERIA web site.³ An analysis of historic data from 2009 to 2016 has shown that the forecast tools have a low FAR (~30%) and a high POD (63%).

The HESPERIA UMASEP-500 model makes real-time predictions of the occurrence of >500 MeV SEP and GLE events from the analysis of SXR and differential proton flux measured by the GOES satellite network. Real-time predictions are available in the HESPERIA web site.⁴ We assume that a prediction is successful when it is reported before the first GLE alert is issued by any NM station. Regarding the prediction of GLE events for the period 2000–2016, this tool had a POD of 53.8%, and a FAR of 30.0%. For this period, the tool obtained an AWT of 8 min taking as reference the alert time from the first NM station; taking as reference the time of the warnings issued by the GLE Alert Plus for the aforementioned period, the HESPERIA UMASEP-500 tool obtained an AWT of 15 min.

In summary, the goal of the presented tools has been to improve mitigation of adverse effects both in space and in the air from a significant solar radiation storm, providing valuable added minutes of forewarning to space weather users.

References

- Chertok, I., Grechnev, V., Meshalkina, N.: On the correlation between spectra of solar microwave bursts and proton fluxes near the Earth. *Astron. Rep.* **53**, 1059–1069 (2009)
- Dennis, B.R., Zarro, D.: The neupert effect – what can it tell us about the impulsive and gradual phases of solar flares? *Sol. Phys.* **146**, 177–190 (1993)
- Dierckxsens, M., Tziotziou, K., Dalla, S., Patsou, I., Marsh, M., Crosby, N.: Relationship between solar energetic particles and properties of flares and CMEs: statistical analysis of solar cycle 23 events. *Sol. Phys.* **290**, 841–874 (2015)
- Grechnev, V., Kiselev, V., Meshalkina, N., Chertok, I.: Relations between microwave bursts and near-earth high-energy proton enhancements and their origin. *Sol. Phys.* **290**, 2827 (2015)
- Holman, G., Aschwanden, H., Aurass, M., Tanaka, S.: Implications of X-ray observations for electron acceleration and propagation in solar flares. *Space Science.* **159**, 107–166 (2011)
- Kahler, S.: The role of the big flare syndrome in correlations of solar energetic proton fluxes and associated microwave burst parameters. *Space Phys.* **87**, 3439–3448 (1982)

³<https://www.hesperia.astro.noa.gr/index.php/results/real-time-prediction-tools/release>

⁴<https://www.hesperia.astro.noa.gr/index.php/results/real-time-prediction-tools/umasep>

- Mewaldt, R., Cohen, C., Mason, G., Cummings, A., Desai, M., Leske, R., Raines, J., Stone, E., Wiedenberck, N., von Rosenvinge, T., Zurbenchen, T.: On the differences in composition between solar energetic particles and solar wind. *Space Sci. Rev.* **130**, 207–219 (2007)
- Müller-Mellin, R.: COSTEP – comprehensive suprathermal and energetic particle analyser. *Sol. Phys.* **162**, 483–504 (1995)
- Nakajima, H., Sekiguchi, H., Sawa, M., Kai, K., Kawashima, S.: The radiometer and polarimeters at 80, 35 and 17 GHz for solar observations at Nobeyama. *Publ. Astron. Soc. J.* **37**, 163–170 (1985)
- Neupert, W.: Comparison of solar X-ray line emission with microwave emission during flares. *Astrophys. J.* **153**, L59–L64 (1968)
- Núñez, M.: Predicting solar energetic proton events ($E > 10$ MeV). *Space Weather.* **9**, S07003 (2011)
- Núñez, M.: Real-time prediction of the occurrence and intensity of the first hours of >100 MeV solar energetic proton events. *Space Weather.* **13**(11), 807–819 (2015)
- Núñez, M., Reyes-Santiago, P., Malandraki, O.E.: Real-time prediction of the occurrence of GLE events. *Space Weather* **15** (2017). doi:[10.1002/2017SW001605](https://doi.org/10.1002/2017SW001605)
- Posner, A.: Up to 1-hour forecasting of radiation hazards from solar energetic ion events with relativistic electrons. *Space Weather.* **5**, S05001 (2007)
- Souvatzoglou, G., Papaioannou, A., Mavromichalaki, H., Dimitroulakos, J., Sarlanis, C.: Optimizing the real-time ground level enhancement alert system based on neutron monitor measurements: introducing GLE Alert Plus. *Space Weather.* **12**(11), 633–649 (2014)
- Torii, C., Tsukiji, Y., Kobayashi, S., Yoshimi, N., Tanaka, H., Enome, S.: Full-automatic radiopolarimeters for solar patrol at microwave frequencies. *Proc. Res. Inst. Atmos.* **26**, 129–132 (1979)
- Trottet, G., Samwel, S., Klein, K., Dudok de Wit, T., Miteva, R.: Statistical evidence for contributions of flares and coronal mass ejections to major solar energetic particle events. *Sol. Phys.* **290**(3), 819–839 (2015)
- Zucca, P., Núñez, M., Klein, K.: Exploring the potential of microwave diagnostics in SEP forecasting: I. The occurrence of SEP events. *J. Space Weather Space Clim.* **7**, 15 (2017)

Open Access This chapter is licensed under the terms of the Creative Commons Attribution 4.0 International License (<http://creativecommons.org/licenses/by/4.0/>), which permits use, sharing, adaptation, distribution and reproduction in any medium or format, as long as you give appropriate credit to the original author(s) and the source, provide a link to the Creative Commons license and indicate if changes were made.

The images or other third party material in this chapter are included in the chapter's Creative Commons license, unless indicated otherwise in a credit line to the material. If material is not included in the chapter's Creative Commons license and your intended use is not permitted by statutory regulation or exceeds the permitted use, you will need to obtain permission directly from the copyright holder.

